Mechanics of Advanced Composite Structures 12 (2025), Serial Number 26, 671 – 683

Semnan University

Mechanics of Advanced Composite Structures

Journal homepage: https://macs.semnan.ac.ir/

ISSN: 2423-7043

Research Article

Effects of Cooling Conditions and Machining Parameters on Thrust Force, Surface Roughness, and Hole Quality in Machining of Fiber Metal Laminates

Meisam Khademitab, Vahid Abedini *, Alireza Hajialimohamadi

Faculty of Mechanical Engineering, Semnan University, Semnan, Iran, P.O. Box: 35131-19111, Iran

ARTICLE INFO

Article history:

Received: 2022-12-14

Revised: 2025-04-16

Accepted: 2025-05-14

Keywords:

Fiber metal laminates;

Thrust forces;

Twist drilling;

Helical milling;

Minimum Quantity Lubrication (MQL).

ABSTRACT

The machining of Fiber Metal Laminates (FMLs), such as glass laminate aluminum reinforced epoxy (GLARE), presents significant challenges due to the varying mechanical and thermal properties of its constituent materials. This study investigates the effects of cooling conditions and machining parameters on thrust force, surface roughness, and hole quality in FMLs. A comparative analysis of two hole-making techniques—twist drilling and helical milling—is performed on two thicknesses of GLARE, under both Minimum Quantity Lubrication (MQL) and dry conditions. The experimental work utilized the Response Surface Methodology (RSM) to assess the impact of spindle speed, feed rate, and cooling conditions on thrust force, torque, surface roughness, and hole quality. Results show that helical milling significantly reduces thrust force by 66% to 81% compared to twist drilling, although it requires a 300% increase in machining time. MQL was effective in decreasing thrust force and surface roughness in both methods. The thicker GLARE samples experienced a 17% to 32% increase in thrust force, leading to higher surface roughness. Spindle speed influenced thrust force by up to 60.68% in twist drilling, whereas feed rate showed the most significant effect (64.19%) in helical milling. This study highlights the advantages of helical milling in reducing machining forces and improving surface quality, despite its longer process time. The results provide useful information for machine configuration optimization, particularly for aerospace applications that frequently use FMLs like GLARE.

1. Introduction

Fiber Metal Laminates (FMLs) are hybrid metallic composites composed of alternating thin metal sheets and intermediate fiber layers bonded with adhesive epoxy [1]. The three primary types of FMLs include ARALL (aramid-reinforced aluminum laminates), CARALL (carbon-reinforced aluminum laminates), and GLARE (glass-reinforced aluminum laminates) [2]. Compared to their components, these materials exhibit superior mechanical properties, such as a high strength-to-weight ratio, enhanced fatigue life, and resistance to fracture propagation, corrosion, and fire [1,3]. The two most common traditional methods for creating holes in these materials are twist drilling and helical milling. A major challenge in drilling hybrid materials is the frequent change in material phases. The metal and fiber layers'

* **Corresponding author.**
E-mail address: v.abedini@semnan.ac.ir

Cite this article as:

Khademitab, M., abedini, V. and hajialimohammadi, A., 2025. Effects of Cooling Conditions and Machining Parameters on Thrust Force, Surface Roughness, and Hole Quality in Machining of Fiber Metal Laminates. *Mechanics of Advanced Composite Structures*, 12(3), pp. 671-683.

https://doi.org/10.22075/MACS.2025.29297.1460

mechanical and thermal conductivity characteristics are markedly different, significantly influencing machining conditions, hole quality, and tool life [4,5]. Brinksmeier et al. [6] investigated heat generation and its impact on the quality of holes in CFRP (carbon fiber reinforced plastics) and CFRP/Ti/Al stacks, finding that helical milling reduces forces, temperature, and surface roughness compared to twist drilling. Voss et al. [7] compared two traditional hole-making processes on CFRP made from prepreg unidirectional carbon fiber. Their results indicated that an increase in the number of holes exacerbates the issue of uncut fibers in twist drilling; specifically, the thrust force in twist drilling reached 210 N, whereas it was only 66 N in helical milling. Geier et al. [8] explored twist drilling of UD-CFRP, highlighting its effectiveness in reducing thrust force, surface roughness, and delamination. They found that the feed rate had a greater influence on thrust force than spindle speed, although both factors significantly impacted surface roughness, with milling pitch having the most considerable effect during helical milling. Wang et al. [9] examined two-step drilling of CFRP/Al stacks and reported that helical milling produced 35% less thrust force than twist drilling, with both processes demonstrating a 25% reduction in thrust force during the second machining stage. Qin et al. [10] studied helical milling in CFRP and found that higher spindle speeds, lower feed rates, and appropriate helical pitch significantly reduced surface delamination. Sadek et al. [11] reported that helical milling decreased thrust force by 45% compared to conventional twist drilling, with no observable surface delamination. They noted that the temperature in the machining zone during tool exit was 60% lower than in twist drilling. Chen et al. [12] compared helical milling using specialized end mills versus standard end mills on CFRP and titanium, finding that the specialized tool produced lower thrust forces on titanium, which resulted in reduced burr formation. Although thrust force reduction on CFRP was minimal, delamination decreased. Tyczynski et al. [13] studied twist drilling on various materials, including CFRP, GFRP (glass fiber reinforced plastics), aluminum, and GLARE, concluding that higher feed rates increased thrust forces and visible damage, with Al 2024-T3 exhibiting the maximum thrust force and MD-CFRP the minimum. Giasin et al. [14] investigated the effects of spindle speed and feed rate on hole size, entrance and exit burr height, delamination, and circularity error using scanning electron microscopy (SEM). They found that good hole quality could be achieved at spindle speeds of 300 mm/min and 3000 rpm. In another study, Giasin et al. [15] examined the effects of three types of cutting tool coatings—TiAlN, AlTiN/TiAlN, and TiN—on burr formation and surface roughness of GLARE holes. Their results indicated that tool coating significantly influenced burr height and thickness, with spindle speed and cutting tool type having the greatest impact on surface roughness. Hemant et al. [16] explored the effects of helical milling on GLARE, made from aluminum 8090 and UD-GF sheets bonded with epoxy. They found that helical pitch had the most significant effect on thrust force, accounting for 58.22%, followed by spindle speed at 37.57%. Spindle speed also notably influenced surface roughness, contributing 75.96%, with feed rate contributing 20.18%. Giasin et al. [17] studied the effects of cryogenic cooling through the tool and drilling parameters on circularity, hole size, surface roughness, and hardness in machining GLARE laminates. Their findings indicated that cryogenic cooling improved the surface finish of holes and enhanced hole size at the top, although it did not affect circularity. Köklü et al. [18] conducted a comparative study of three materials—carbon/epoxy, glass/epoxy, and functionally graded composites (FGC)—during drilling processes, analyzing the effects of drilling parameters on roundness, delamination, hole diameter, and thrust force. They demonstrated that drilling FGC is more complex than drilling glass/epoxy and carbon/epoxy. Köklü et al. [19] also examined the impact of drilling S2 glass fiber composites in an LN2 bath, aiming to determine how spindle speed, feed rate, and cryogenic cooling affect hole shape and dimensional tolerances. Their experimental design and analysis of variance revealed that drilling S2 glass fiber in a cryogenic bath resulted in significantly larger holes than the nominal diameter. While the existing literature emphasizes the influence of various machining parameters and cooling conditions on thrust force, surface roughness, and hole quality in FMLs, the current study offers several unique contributions:

This study provides a direct comparative analysis between two prevalent hole-making methods—twist drilling and helical milling—under a variety of cooling conditions. By investigating the impact of Minimum Quantity Lubrication (MQL) alongside traditional dry conditions, the study highlights the interactions between cooling conditions and machining parameters. This contributes to a more comprehensive understanding of how cooling conditions affect thrust force and surface quality during the machining of FMLs. In addition, the research involves specimens of varying thicknesses, enhancing the understanding of how material properties and dimensions influence machining performance.

2. Materials and Methods

The workpiece material is a type of hybrid composite material called FMLs. The layers consisted of anodized thin aluminum sheets (0.7 mm thickness) and UD-GF that were bonded together by resin epoxy solidly. The aluminum is 2024-T3, which has excellent mechanical properties and good machinability. The surface of aluminum plates must be textured to produce maximum bonding with the epoxy resin. Thin-Film Sulphuric Acid Anodizing (TFSAA) is used for this purpose. Aluminum plates are anodized in a 5% by weight sulfuric acid (H2SO4) solution. The voltage increases from 3 to 15 volts per minute, remaining constant for 20 minutes [20, 21]. The specimens manufactured by the hand lay-up process assisted by a vacuum bag molding are shown in Fig. 1. This method gives the best result because it reduces micro-gaps between layers and evacuates air and extra resin epoxy from them. The properties of the material are shown in Table 1.

Table 1. Mechanical Properties of Materials [3, 22]

Mechanical property	Al2024-T3	E-Glass	Epoxy LG 735 G	Units
Young Modulus	72.2	71	-	GPa
Ultimate tensile strength	455	2275	56-78	MPa
Ultimate strain (%)	19	4.8	1.5-2.5	GPa
Shear Modulus	27.6	30	-	GPa
Poisson's ratio	0.33	0.2	-	GPa
Density	2770	2560	1180	kg/m^3
Thermal conductivity	121	1.03	-	W/m-K

The specimens have been made in two different thicknesses, like GLARE 2B (LGB). The UGF has a 90-degree angle with the direction of rolling aluminum. The first is made of eight aluminum layers and seven duplicated UGFs called LGB8/7 with 9.3 mm thickness; the second is made of three aluminum layers and two repeated UGFs called LGB3/2 with 3 mm thickness. The workpiece dimension is 200 x 150 mm.

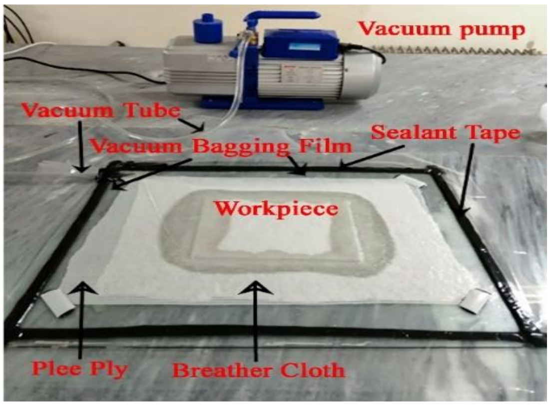

Fig. 1. Hand Lay-Up Method and the Use of the Vacuum Bagging Process

Two tools are used to make the holes: the twist drill and the four-flute coated carbide end mill. The results of recent research show that tools coated with TiAlN (titanium aluminum nitride) have good wear resistance at higher temperatures. Specifications of the tools are shown in Table 2.

Table 2. Specifications for the Twist Drill and End Mill

	Twist Drill	End mill
Material	Solid carbide	Solid carbide
Coating	TiAlN- coating thickness 4µm	TiAlN-coating thickness 4µm
Helical pitch	30 degree	45 degree
Number of Flutes	2	4
Point Angle	120	-
Dimensions	66× Φ6 mm	50× Φ4 mm

A WABECO CC F-100 (PC - F426-2) three-axis computer numerical control (CNC) milling machine with a 2.2 KW spindle and 7500 rpm is used to drill holes. A fixture clamps the workpiece to a dynamometer as a backup plate. Fig.2 presents the experimental setup process.

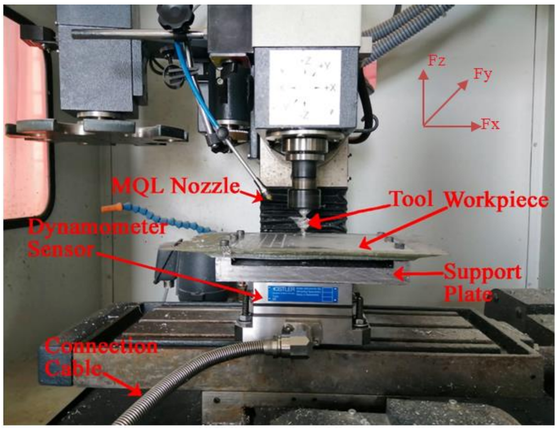

Fig. 2. The Machining Setup

Minimum Quantity Lubrication (MQL) is used in this study. The MQL system can supply the coolant mixed with small amounts of compressed air under pressures ranging from 1 to 4 bars to produce coolant flow rates between 20 and 600 ml/hr. The nozzle has a small hole with a 1.2 mm diameter at the end and is located 8 cm from the tool's tip with a 30-degree angle to the tool's axis. The coolant liquid is a natural oil called Easy Cut. The Kistler dynamometer type 9257B measures the forces with a frequency of 1000 Hz during the machining process. Measuring the hole surface roughness is an effective way to consider the hole quality. For each hole, surface roughness is measured in four different sections and the same direction, situated around the internal hole wall at 0, 90, 180, and 270 degrees to reduce the impact of fiber orientation on the final surface roughness. A portable Mahr PS1 is used to measure the average roughness Ra. Response surface method (RSM) is used for the design of the experiment (DOE) to determine the influence of the spindle speeds, the feed rate, and cooling conditions (MQL and Dry) on the forces and surface roughness. This study included 19 trials based on machining parameters. Analysis of variance (ANOVA) via Design-Expert®11 software was carried out to determine the contribution percentage of spindle speed, feed rate, and cooling conditions, and their interaction on the results. Table 3 shows the details of the experiments. A schematic of the process steps is explained in Fig. 3.

Table 3. Experiments Designed Using Response Surface Methodology (RSM)

Run	Spindle speed (RPM)	Feed rate (mm/min)	Cooling conditions
1	3000	150	MQL
2	3000	150	DRY
3	3000	50	MQL
4	2000	50	MQL
5	2000	50	DRY
6	2000	100	MQL
7	1000	150	MQL
8	2000	50	DRY
9	1000	50	MQL
10	1000	100	MQL
11	3000	100	MQL
12	2000	150	DRY
13	3000	100	DRY
14	2000	100	MQL
15	2000	100	MQL
16	1000	100	DRY
17	1000	50	DRY
18	2000	150	DRY
19	1000	100	DRY

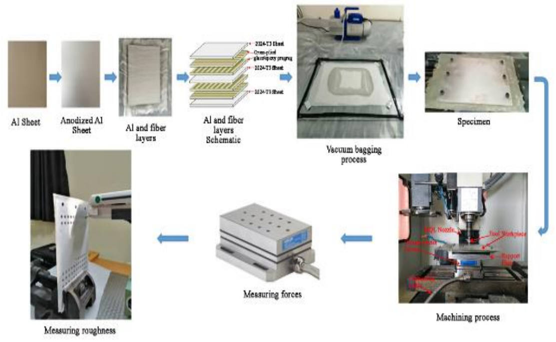

Fig. 3. Schematic Representation of the Process Steps

3. Results and Discussion

3.1. Analysis of Thrust Forces and Torques

A comparison was carried out between twist drilling and helical milling for the LGB3/2 workpiece in terms of thrust force (Fz). The results revealed that helical milling reduced thrust force from 61% to 81% compared to twist drilling. This decrease in thrust force can be attributed to two primary factors. Firstly, in helical milling, the tool's diameter is smaller than the final hole diameter, enabling efficient coolant penetration to the machining area and thereby reducing friction in the machining zone. Secondly, the end mill tool's cutting edges are located at the tip and its surrounding area, generating a helical milling chip with multiple cutting edges. As a result, forces are distributed in three directions (Fz, Fx, Fy), leading to a lower intensity of thrust force compared to twist drilling.

Furthermore, the influence of thickness on thrust force was also examined in the twist drilling process. The findings demonstrated that thicker workpieces resulted in a thrust force increase of 17% to 32% compared to thinner ones. This phenomenon can be explained by two main factors. Firstly, thicker workpieces hinder the quick evacuation of chips, resulting in counteractive forces. Secondly, the tool makes more contact with the internal wall of the hole as the workpiece thickness increases, causing additional friction and subsequently leading to higher thrust force. Fig. 4 shows the thrust force changes based on the workpiece and process.

Tables 4 and 5 present the outcomes of the Analysis of Variance (ANOVA) for the thrust force during both twist drilling and helical milling processes on the LGB3/2 workpiece. Table 4 indicates that spindle speed has the most significant impact, accounting for 60.68% of the variation in thrust force. In comparison, the feed rate contributes 37.4% to this variation, while the combined effect of their interaction on thrust force is relatively minor.

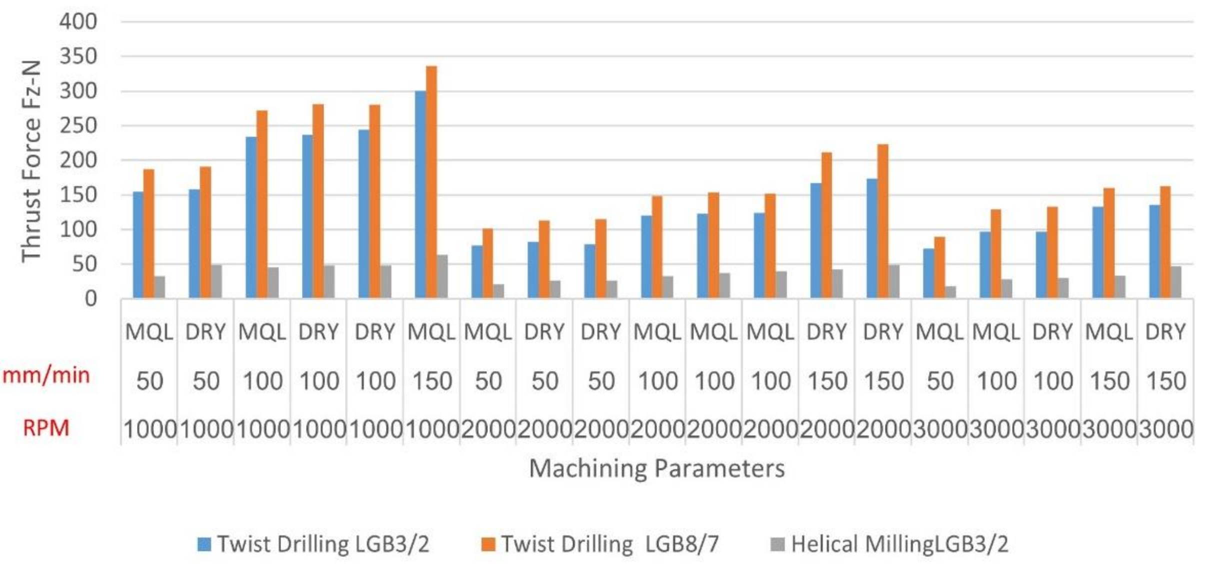

Fig. 4. Thrust Forces and Their Variations Due to Different Processes and Machining Parameters

Table 4. ANOVA Analysis of Thrust Force During the Twist Drilling Process on the LGB3/2

Source	Sum of Squares	df	Mean Square	F-value	p-value	
Model	119.16	4	29.79	686.78	< 0.0001	significant
A-Spindle speed	72.31	1	72.31	1667.11	< 0.0001	
B-Feed rate	44.57	1	44.57	1027.47	< 0.0001	
AB	1.18	1	1.18	27.11	0.0001	
A^2	10.92	1	10.92	251.70	< 0.0001	
Residual	0.6073	14	0.0434			
Lack of Fit	0.5141	9	0.0571	3.07	0.1150	not significant
Pure Error	0.0932	5	0.0186			
Cor Total	119.77	18				

Table 5. ANOVA Analysis of Thrust Force During the Helical Milling Process on the LGB3/2

Source	Sum of Squares	df	Mean Square	F-value	p-value	
Model	14.19	2	7.10	45.70	< 0.0001	significant
A-Spindle speed	7.61	1	7.61	49.01	< 0.0001	
B-Feed rate	9.09	1	9.09	58.55	< 0.0001	
Residual	2.49	16	0.1553			
Lack of Fit	2.22	11	0.2016	3.77	0.0773	not significant
Pure Error	0.2677	5	0.0535			
Cor Total	16.68	18				

The impacts of twist drilling and helical milling on the LGB3/2 workpiece are contrasted in Table 5, which shows that the feed rate has a greater impact (64.19%) than the spindle speed (53.62%). Notably, there is no statistically significant interaction between these parameters.

Figure 5 further supports these findings by illustrating a 3D response contour plot that depicts the interaction between spindle speed and feed rate on thrust force (Fz), thereby corroborating the earlier explanations.

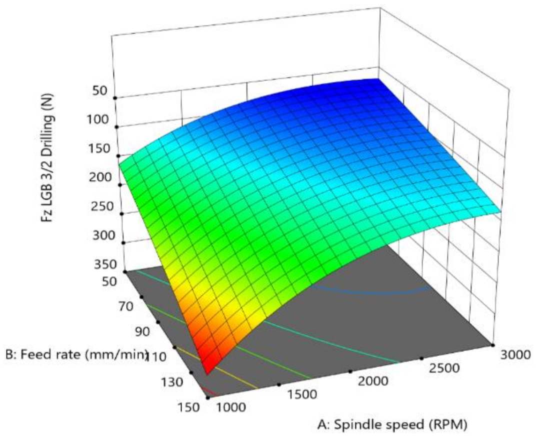

(a)

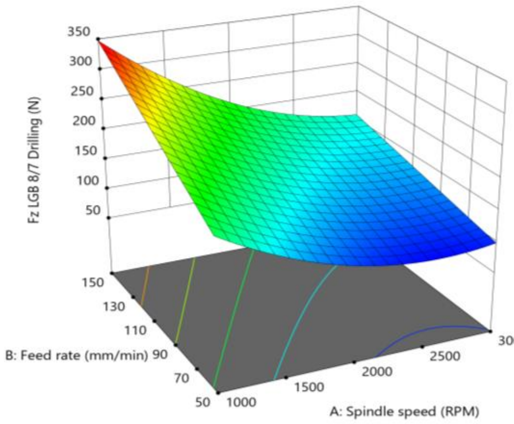

(b)

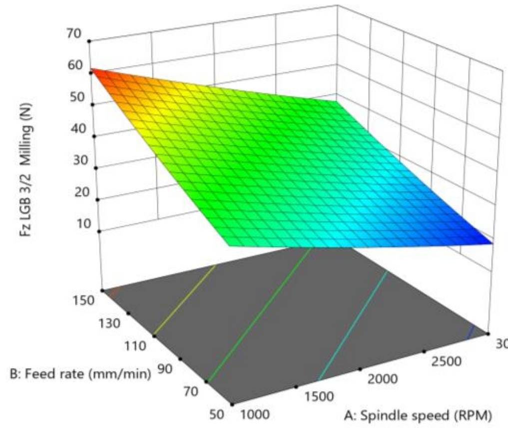

(c)

Fig. 5. 3D Response Contour Plot Showing the Interaction Between Spindle Speed and Feed Rate on Thrust Force (Fz) Under Dry Conditions: (a) Twist Drilling with LGB3/2, (b) Twist Drilling with LGB8/7, (c) Helical Milling with LGB3/2

In the context of twist drilling, torque emerges as a significant factor. The findings illustrate that augmenting the feed rate while maintaining a consistent spindle speed results in an increase in torque for both workpiece thicknesses. This effect can be attributed to the rise in feed rate, leading to an increase in the thickness of the uncut chips. Additionally, the accelerated feed rate provides the cutting tool with less time to create thicker chips, thereby giving rise to heightened torque levels. The torque values of the LGB8/7 exceed those of the LGB3/2 by 14.5% to 31%. This phenomenon is primarily driven by the escalating depth of holes in the thicker workpiece. Consequently, there is a greater degree of contact and friction between the hole's walls and the tool, thereby causing an increase in torque. Upon analyzing the torque data for the LGB8/7, it is apparent that the minimum torque value occurs at a spindle speed of 3000 rpm and a feed rate of 50 mm/min, registering at 0.667 N.m. Conversely, the maximum torque is observed at a spindle speed of 1000 rpm and a feed rate of 150 mm/min, measuring 1.804 N.m. In the case of the LGB3/2, the maximum torque materializes at a spindle speed of 1000 rpm and a feed rate of 150 mm/min, amounting to 1.333 N.m. Conversely, the minimum torque value is recorded at a spindle speed of 3000 rpm and a feed rate of 50 mm/min. Figure 6 visually depicts the fluctuations in torque following the machining parameters.

Tables 6 and 7 present the outcomes of the Analysis of Variance (ANOVA) for the torque response in both the LGB3/2 and LGB8/7 workpieces during twist drilling. In the ANOVA results for twist drilling on the LGB3/2, it is evident that the spindle speed, identical to that of the LGB8/7, significantly impacts torque by 58.28%, followed by the feed rate contributing 41.92%. The interaction percentage between spindle speed and feed rate, with a 3.15% influence on torque, remains insignificant. Additionally, the Minimum Quantity Lubrication (MQL) condition has a modest effect, contributing only 1.53% to torque variation. In the case of the ANOVA performed on the LGB8/7, the findings demonstrate that the spindle speed carries a substantial influence, contributing to 59.01% of the torque variation, followed by the feed rate with a contribution of 38.55%. Similarly, the MQL condition has a minor impact of 2% on the torque variation. Figure 7 complements these results by illustrating a 3D response contour plot, portraying the interaction between spindle speed and feed rate on torque under dry conditions.

Fig. 6. Variations in Torque During Twist Drilling Based on Machining Parameters

Table 6. ANOVA Analysis of Torque During the Twist Drilling Process on the LGB3/2

Source	Sum of Squares	df	Mean Square	F-value	p-value	
Model	1.01	6	0.1684	50.66	< 0.0001	significant
A-Spindle speed	0.5928	1	0.5928	178.32	< 0.0001	
B-Feed rate	0.4235	1	0.4235	127.41	< 0.0001	
C-Condition	0.0155	1	0.0155	4.67	0.0517	
AB	0.0319	1	0.0319	9.59	0.0092	
A^2	0.0282	1	0.0282	8.48	0.0130	
B^2	0.0178	1	0.0178	5.37	0.0390	
Residual	0.0399	12	0.0033			
Lack of Fit	0.0193	7	0.0028	0.6667	0.6985	not significant
Pure Error	0.0206	5	0.0041			
Cor Total	1.05	18				

Table 7. ANOVA Analysis of Torque During the Twist Drilling Process on the LGB8/7

Source	Sum of Squares	df	Mean Square	F-value	p-value	
Model	0.3548	6	0.0591	108.99	< 0.0001	significant
A-Spindle speed	0.2094	1	0.2094	385.86	< 0.0001	
B-Feed rate	0.1368	1	0.1368	252.16	< 0.0001	
C-Condition	0.0069	1	0.0069	12.69	0.0039	
AB	0.0038	1	0.0038	6.94	0.0218	
A^2	0.0260	1	0.0260	47.86	< 0.0001	
B^2	0.0098	1	0.0098	18.07	0.0011	
Residual	0.0065	12	0.0005			
Lack of Fit	0.0055	7	0.0008	3.97	0.0743	not significant
Pure Error	0.0010	5	0.0002			
Cor Total	0.3613	18				

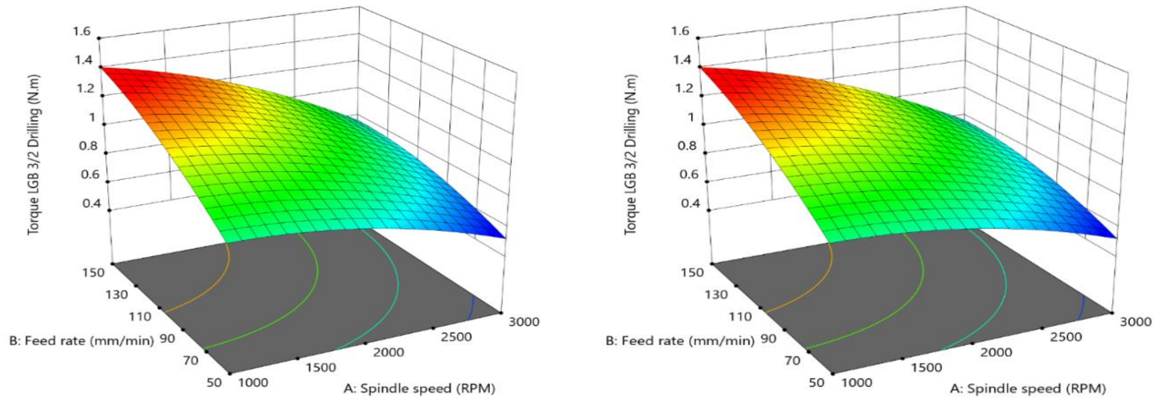

Fig. 7. 3D Response Contour Plot Illustrating the Interaction Between Spindle Speed and Feed Rate on Torque under Dry Conditions: (a) Twist Drilling with LGB3/2, (b) Twist Drilling with LGB8/7

3.2. Analysis of Surface Roughness

Figure 8 depicts the average value of surface roughness (Ra) obtained from the experiments. In the context of twist drilling for both workpieces, elevating the feed rate while maintaining a constant spindle speed increases surface roughness. A comparison between the LGB3/2 and LGB8/7 workpieces reveals that the surface roughness in the LGB8/7 is elevated by 1% to 41% compared to the LGB3/2. The highest Ra is recorded at a spindle speed of 1000 rpm and a feed rate of 150 mm/min, amounting to 3.371 µm for the LGB8/7 and 3.317 µm for the LGB3/2.

Three primary reasons could account for the disparities in surface roughness. Firstly, in the case of the thicker workpiece, the hole's greater depth prolongs chip evacuation time, allowing chips more time to impact and damage the hole wall, thereby resulting in heightened surface roughness. Secondly, deeper holes engender more pronounced vibrations between the tool and the hole wall, exacerbating the occurrence of chatter and leading to increased damage to the hole wall. Lastly, the generation of heat is more substantial in deeper holes compared to shallower ones. This elevated heat softens the matrix, causing the fibers to separate more easily from the matrix, consequently leading to a lower surface quality.

A subsequent comparison between twist drilling and helical milling processes on the LGB3/2 workpiece is drawn. The results indicate that the surface roughness achieved through helical milling is notably improved, ranging between 7% and 58%, compared to the outcomes of twist drilling. In helical milling, the applied forces are distributed across two primary directions: the axial force (Fz) and the radial forces (Fx, Fy). This distribution pattern results in a lower concentration of axial force in comparison to twist drilling. As a consequence, the temperature in the machining zone decreases, leading to enhanced surface roughness. Additionally, owing to the 2mm disparity between the hole and tool diameter in helical milling, chips can evacuate more effectively than in twist drilling. The efficient removal of chips reduces potential damage to the hole wall, therefore aiding in the decrease of surface roughness during helical milling.

The highest recorded surface roughness occurs at a spindle speed of 1000 rpm and a feed rate of 150 mm/min. Specifically, in the case of helical milling, the maximum surface roughness measures 1.532 µm, whereas for twist drilling, it is 3.317 µm.

An overview of the surface roughness response's Analysis of Variance (ANOVA) results is given in Tables 8 through 10. For twist drilling on the LGB3/2, the ANOVA reveals that spindle speed exerts the most significant impact, accounting for a maximum effect of 50.07% on surface roughness, closely followed by the feed rate with a contribution of 35.66%. Turning to the LGB8/7 analysis, spindle speed emerges as the dominant factor, influencing surface roughness by 61.14%, trailed by the feed rate at 32.28%. Moreover, the interaction between spindle speed and feed rate exhibits a 6.55% influence on surface roughness.

Further inspecting of the ANOVA results for helical milling, the findings highlight the substantial influence of spindle speed, accounting for 77.7% of the surface roughness variation, accompanied by the feed rate contributing 38.7%. It's worth noting that increasing the feed rate while maintaining a constant spindle speed leads to elevated surface roughness. The most significant differences in surface roughness, reaching up to 27%, are observed at a spindle speed of 1000 rpm and a feed rate of 150 mm/min. Notably, the disparities are 22% and 18% at constant spindle speeds of 2000 rpm and 3000 rpm, respectively. To visually capture the interaction between spindle speed and feed rate on surface roughness under Minimum Quantity Lubrication (MQL) conditions, Figure 9 portrays a 3D response contour plot.

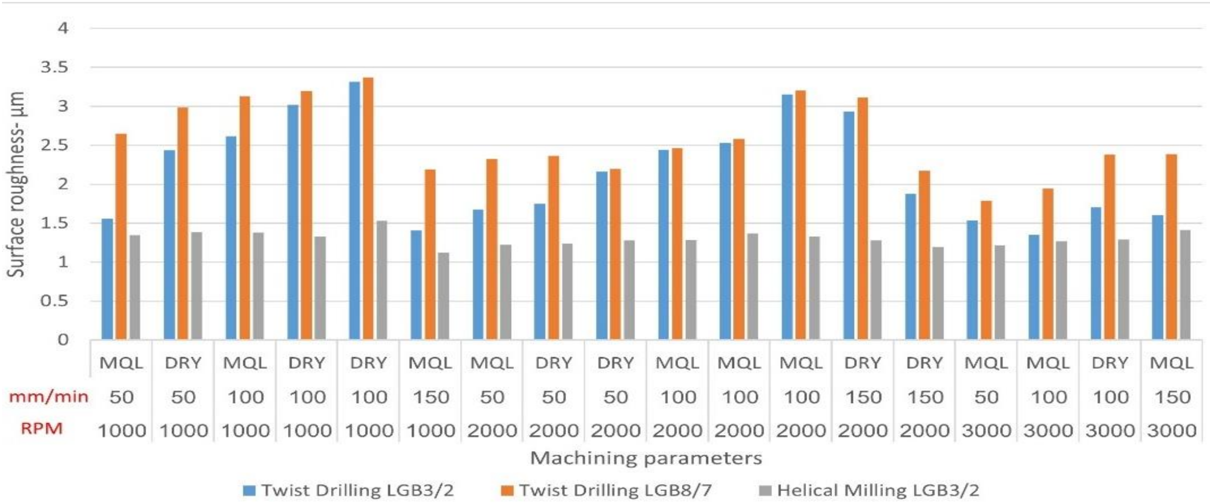

Fig. 8. Variations in Surface Roughness

Table 8. ANOVA Analysis of Surface Roughness During the Twist Drilling Process on the LGB3/2

Source	Sum of Squares	df	Mean Square	F-value	p-value	
Model	6.87	5	1.37	23.10	< 0.0001	significant
A-Spindle speed	2.45	1	2.45	41.28	< 0.0001	
B-Feed rate	3.44	1	3.44	57.84	< 0.0001	
C-Condition	0.0404	1	0.0404	0.6796	0.4246	
AB	1.75	1	1.75	29.51	0.0001	
AC	0.2161	1	0.2161	3.63	0.0790	
Residual	0.7729	13	0.0595			
Lack of Fit	0.5946	8	0.0743	2.08	0.2174	not significant
Pure Error	0.1783	5	0.0357			
Cor Total	7.64	18				

Table 9. ANOVA Analysis of Surface Roughness During the Twist Drilling Process on the LGB8/7

Source	Sum of Squares	df	Mean Square	F-value	p-value	
Model	3.50	4	0.8738	28.32	< 0.0001	significant
A-Spindle speed	2.14	1	2.14	69.47	< 0.0001	
B-Feed rate	1.27	1	1.27	41.27	< 0.0001	
C-Condition	0.2135	1	0.2135	6.92	0.0198	
AB	0.2295	1	0.2295	7.44	0.0164	
Residual	0.4319	14	0.0309			
Lack of Fit	0.3452	9	0.0384	2.21	0.1980	not significant
Pure Error	0.0867	5	0.0173			
Cor Total	3.93	18				

Table 10. ANOVA Analysis of Surface Roughness During the Helical Milling Process on the LGB3/2

Source	Sum of Squares	df	Mean Square	F-value	p-value	
Model	0.1000	2	0.0500	13.32	0.0004	significant
A-Spindle speed	0.0387	1	0.0387	10.31	0.0055	
B-Feed rate	0.0777	1	0.0777	20.70	0.0003	
Residual	0.0601	16	0.0038			
Lack of Fit	0.0524	11	0.0048	3.11	0.1102	not significant
Pure Error	0.0077	5	0.0015			
Cor Total	0.1601	18				

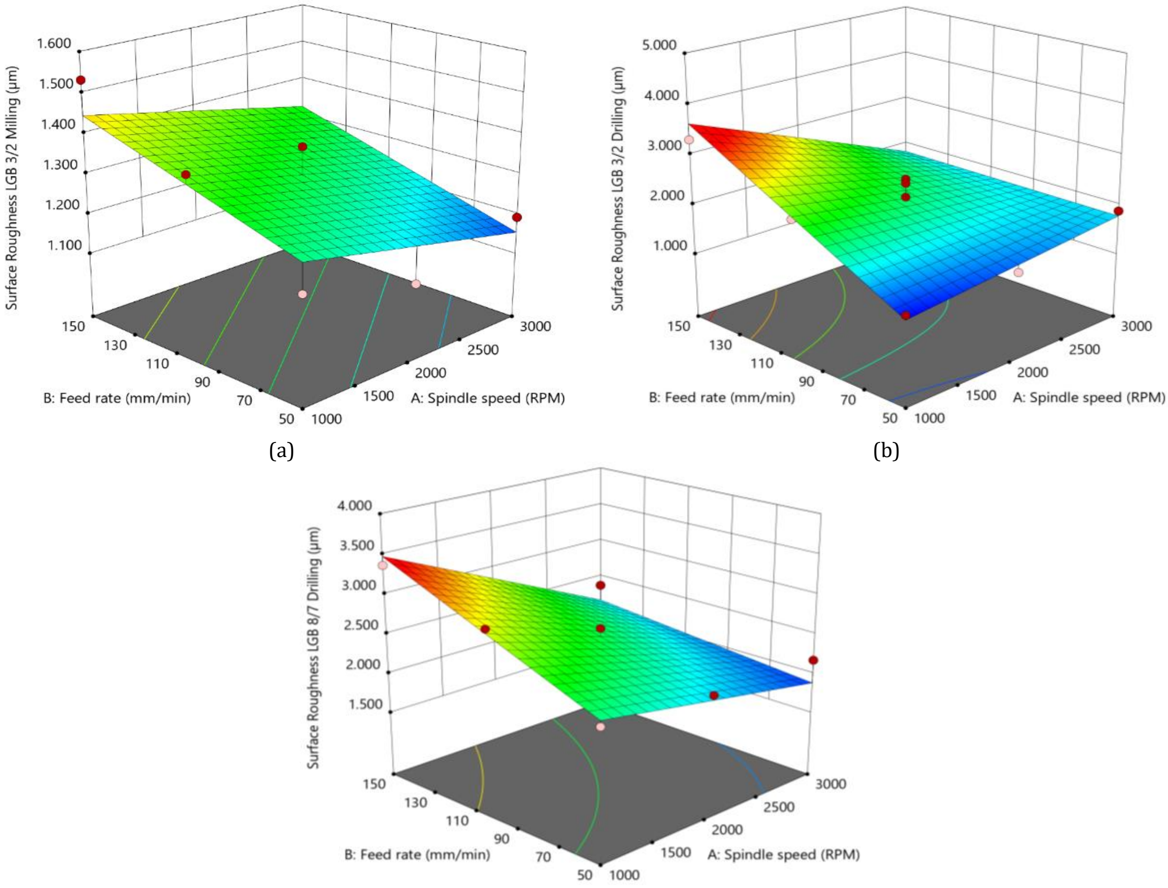

Fig. 9. 3D Response Contour Plot Showing the Interaction Between Spindle Speed and Feed Rate on Surface Roughness Under MQL Conditions: (a) Helical Milling with LGB3/2, (b) Twist Drilling with LGB3/2, (c) Twist Drilling with LGB8/7

3.3. Analysis of Hole Size

The LGB8/7 specimen is selected to show how different machining conditions affect hole size. The results show that the machining condition significantly influences the size of the hole. The top and bottom diameters of the holes are measured, and the results in Fig. 10 show that both sides have slightly risen in diameter when the feed rate was raised at the same spindle speed. However, at the same feed rate, by increasing the spindle speed, the diameter of the holes has no specific changes on both sides. The results show that the bottom diameter has a minor deviation from the nominal size compared to the top diameter. Because FMLs are made like composites, some portions of the specimen have a lower fiber density, affecting the machining condition and outcomes. Furthermore, the specimen reacted elastically due to the high feed rate (150 mm/min), and after the machining process, it returned to the shape it had before drilling.

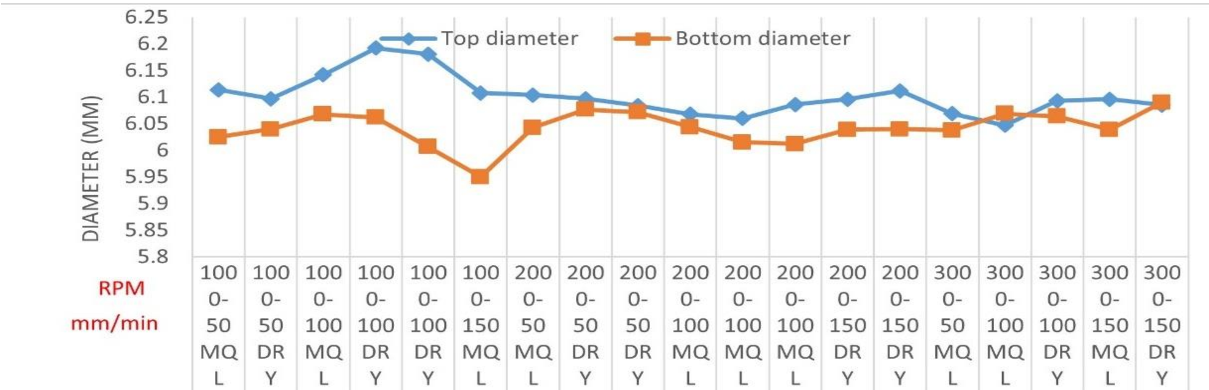

RPM mm/min	1000-50 MQL	1000-50 DRY	1000-100 MQL	1000-100 DRY	1000-100 DRY	1000-150 MQL	2000-50 MQL	2000-50 DRY	2000-50 DRY	2000-100 MQL	2000-100 MQL	2000-100 MQL	2000-150 DRY	2000-150 DRY	3000-50 MQL	3000-100 MQL	3000-100 DRY	3000-150 MQL	3000-150 DRY
Top diameter	6.11	6.1	6.14	6.19	6.18	6.11	6.1	6.1	6.08	6.07	6.06	6.09	6.1	6.11	6.07	6.05	6.09	6.1	6.09
Bottom diameter	6.03	6.04	6.07	6.06	6.01	5.95	6.04	6.08	6.07	6.04	6.02	6.01	6.04	6.04	6.04	6.07	6.06	6.04	6.09

Fig. 10. Diameter on Both Sides of the LGB 8/7

The response contour plot of the interaction between spindle speed and feed rate (Fig. 11) shows that the best results are achieved at the maximum spindle speed and minimum feed rate, as proven in the other sections of this article. By reducing the feed rate and increasing spindle speed, the size of uncut chips decreases, and as a result, the machining conditions improve.

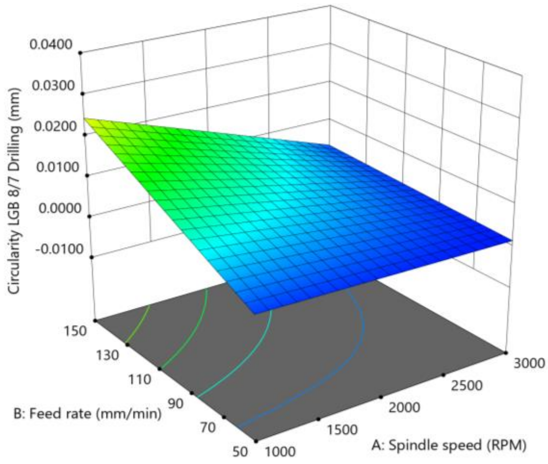

Fig. 11. 3D Response Contour Plot Illustrating the Interaction Between Spindle Speed and Feed Rate

3.4. Effect of Cooling Conditions

The utilization of Minimum Quantity Lubrication (MQL) leads to a reduction in thrust force in both machining processes, with a more pronounced effect observed in helical milling. The decrease in thrust force is comparatively lower in twist drilling. As discussed in the preceding section, the smaller tool diameter in helical milling relative to the final hole diameter enables a greater amount of coolant to access the machining area compared to twist drilling. The examination of the impact of cooling conditions on thrust force, surface roughness, and torque entails analyzing their respective changes within each process.

Upon analyzing the thrust force in twist drilling on the LGB8/7 under MQL conditions, it is determined that the reduction percentage of thrust force falls between 2% and 12%. For the LGB3/2, this reduction ranges from 2% to 5.6%. Conversely, in helical milling, the thrust force reduction spans between 6% and 48%. These results affirm that the reduction in thrust forces is more pronounced in helical milling due to the implementation of the external cooling system. The dissimilarity between the tool and hole diameters in helical milling facilitates a more substantial flow of cooling fluid to the machining area. Analyzing the impact of the MQL condition on torque variations reveals that torque reduction ranges between 0.5% and 17.6% on the LGB3/2 and between 1.2% and 15% on the LGB8/7. Furthermore, improvements in surface roughness are observed, ranging from 0.3% to 12.9% in twist drilling on the LGB8/7 and from 6% to 18% on the LGB3/2. For helical milling on the LGB3/2, changes in surface roughness are found to be between 3.7% and 10.5%.

4. Conclusions

On the LGB3/2, helical milling had a thrust force of 61% to 81 % less than twist drilling, but the machining time was nearly four times longer. The thickness impact on thrust forces in twist drilling revealed that thrust forces on the LGB8/7 were between 17 and 32 percent higher than on the LGB3/2. The friction between the tool and the hole wall increases with thickness, and chip evacuation becomes more difficult, increasing thrust forces. The results of ANOVA in twist drilling on the LGB3/2 showed that the spindle speed had a maximum influence on the thrust force of 60.68%, followed by the feed rate of 37.4%. The same results were obtained on the LGB8/7, with a spindle speed of 59.57% and a feed rate of 34.74%. In helical milling, the feed rate had the highest impact on the thrust force of 64.19%, followed by the spindle speed of 53.62%. Analysis of torque differences during twist drilling on the LGB 3/2 and the LGB8/7 revealed that the torque of the LGB8/7 was between 14.5% and 31% greater than the torque of the LGB3/2.

The ANOVA for twist drilling of the LGB 8/7 Showed that the spindle speed has a major impact of 59.01% on the torque, which was followed by a feed rate of 38.55%, The same Analysis on the LGB3/2 showed spindle speed has a significant effect of 58/28% on the torque, followed by the feed rate of 41.92%. The percentage of the interaction of the spindle speed and the feed rate was insignificant at 3.15% on the torque, and the MQL condition had a mere influence of 1.53% on it.

Surface roughness results showed that twist drilling on the LGB8/7 had between 1% and 41% more surface roughness than the LGB3/2. The maximum surface roughness was measured at the spindle speed of 1000 rpm and feed rate of 150 mm/min. Surface roughness in helical milling was between 7% and 58% lower than twist drilling on the LGB3/2. ANOVA showed that in twist drilling on the LGB3/2 and LGB8/7, the spindle speed had a major effect on the surface roughness of 50.07% and 61.14%, respectively, followed by a feed rate of 35.66% on the LGB3/2 and 32.28% on the LGB8/7. The Analysis of variance for helical milling on the LGB3/2 showed that the spindle speed has a significant influence of 77.7% on the surface roughness, which is followed by the feed rate of 38.7%.

The MQL condition improved all results. The thrust force in twist drilling on the LGB3/2 decreased between 2% and 5.6%, and on the LGB8/7/7the reduction was between 2% and 12%. This reduction for helical milling on the LGB3/2 was between 7% and 48%. The reduction in the torque in twist on the LGB3/2 was between 0.5% and 17.6%, it was between 1.2% and 15% on the LGB8/7. The study of surface roughness demonstrated that twist drilling on the LGB3/2 reduced by 6% to 18%, and the reduction on the LGB8/7 was between 0.3% and 12.9%. In helical milling on the LGB3/2, results showed that the surface roughness reduction was between 3.7% and 10.5%.

Funding Statement

This research did not receive any specific grant from funding agencies in the public, commercial, or not-for-profit sectors.

Conflicts of Interest

The author declares that there is no conflict of interest regarding the publication of this article.

References

[1] Vlot, A. and Gunnink, J.W. eds., 2011. Fibre metal laminates: an introduction. Springer Science & Business Media.

[2] Giasin, K., Hawxwell, J., Sinke, J., Dhakal, H., Köklü, U. and Brousseau, E., 2020. The effect of cutting tool coating on the form and dimensional errors of machined holes in GLARE® fibre metal laminates. The International Journal of Advanced Manufacturing Technology, 107, pp. 2817-2832.

[3] Giasin, K., 2018. The effect of drilling parameters, cooling technology, and fiber orientation on hole perpendicularity error in fiber metal laminates. The International Journal of Advanced Manufacturing Technology, 97, pp. 4081-4099.

[4] Giasin, K. and Ayvar-Soberanis, S., 2017. Microstructural investigation of drilling-induced damage in fibre metal laminates constituents. Composites Part A: Applied Science and Manufacturing, 97, pp. 166-178.

[5] Giasin, K. and Ayvar-Soberanis, S., 2017. An Investigation of burrs, chip formation, hole size, circularity and delamination during drilling operation of GLARE using ANOVA. Composite Structures, 159, pp. 745-760.

[6] Brinksmeier, E., Fangmann, S. and Rentsch, R., 2011. Drilling of composites and resulting surface integrity. CIRP annals, 60(1), pp. 57-60.

[7] Voss, R., Henerichs, M. and Kuster, F., 2016. Comparison of conventional drilling and orbital drilling in machining carbon fibre reinforced plastics (CFRP). Cirp Annals, 65(1), pp. 137-140.

[8] Geier, N. and Szalay, T., 2017. Optimisation of process parameters for the orbital and conventional drilling of uni-directional carbon fibre-reinforced polymers (UD-CFRP). Measurement, 110, pp. 319-334.

[9] Wang, G.D., Melly, S.K. and Li, N., 2018. Experimental studies on a two-step technique to reduce delamination damage during milling of large diameter holes in CFRP/Al stack. Composite Structures, 188, pp. 330-339.

[10] Qin, X., Wang, B., Wang, G., Li, H., Jiang, Y. and Zhang, X., 2014. Delamination analysis of the helical milling of carbon fiber-reinforced plastics by using the artificial neural network model. Journal of Mechanical Science and Technology, 28, pp. 713-719.

[11] Sadek, A., Meshreki, M. and Attia, M.H., 2012. Characterization and optimization of orbital drilling of woven carbon fiber reinforced epoxy laminates. CIRP annals, 61(1), pp. 123-126.

[12] Chen, Q.L., Chen, X.M., Duan, Z.H. and Cun, W.Y., 2015. Research on helical milling specialized tools based on the chip-splitting mechanism. Advanced Materials Research, 1061, pp. 497-506.

[13] Tyczyński, P., Lemańczyk, J., Ostrowski, R. and Ewa S´ liwa, R., 2014. Drilling of CFRP, GFRP, glare type composites. Aircraft Engineering and Aerospace Technology: An International Journal, 86(4), pp. 312-322.

[14] Giasin, K., Ayvar-Soberanis, S., French, T. and Phadnis, V., 2017. 3D finite element modelling of cutting forces in drilling fibre metal laminates and experimental hole quality analysis. Applied Composite Materials, 24, pp. 113-137.

[15] Giasin, K., Gorey, G., Byrne, C., Sinke, J. and Brousseau, E., 2019. Effect of machining parameters and cutting tool coating on hole quality in dry drilling of fiber metal laminates. Composite structures, 212, pp. 159-174.

[16] Hemant, K., Kona, A. and Bolar, G., 2020. Experimental investigation into helical hole

milling of fiber metal laminates. Materials Today: Proceedings, 27, pp. 208-216.

[17] Giasin, K., Dad, A., Brousseau, E., Pimenov, D., Mia, M., Morkavuk, S. and Koklu, U., 2021. The effects of through tool cryogenic machining on the hole quality in GLARE® fibre metal laminates. Journal of Manufacturing Processes, 64, pp. 996-1012.

[18] Köklü, U., Demir, O., Avcı, A. and Etyemez, A., 2017. Drilling performance of functionally graded composite: Comparison with glass and carbon/epoxy composites. Journal of Mechanical Science and Technology, 31, pp. 4703-4709.

[19] Koklu, U., Morkavuk, S., Featherston, C., Haddad, M., Sanders, D., Aamir, M., Pimenov, D.Y. and Giasin, K., 2021. The effect of cryogenic machining of S2 glass fibre composite on the hole form and dimensional tolerances. The International Journal of Advanced Manufacturing Technology, 115(1), pp. 125-140.

[20] Beck, M.E.N., 2003. Performance Validation of Thin-film Sulfuric Acid Anodizatio n (TFSAA) on Aluminum Alloys. Naval Air Systems Command (NAVAIR).

[21] Park, S.Y., Choi, W.J., Choi, H.S., Kwon, H. and Kim, S.H., 2010. Recent trends in surface treatment technologies for airframe adhesive bonding processing: a review (1995–2008). The Journal of Adhesion, 86(2), pp. 192-221.

[22] Hartman, D.R., Greenwood, M.E. and Miller, D.M., 1994. High strength glass fibers. Moving Forward With 50 Years of Leadership in Advanced Materials., 39, pp. 521-533.